Integrated Gas Turbine System Diagnostics: Components and Sensor Faults Quantification using Artificial Neural Network

Emmanuel O. Osigwe, Yi-Guang Li, Sampath Suresh and Gbanaibolou Jombo
e.o.osigwe@cranfield.ac.uk
Cranfield University
Power Propulsion Engineering Centre
Cranfield, Bedford
United Kingdom

Dieni Indarti
BP North Sea
Rotating Equipment
Aberdeen
United Kingdom

ABSTRACT

The role of diagnostic systems in gas turbine operations has changed over the past years from a single support troubleshooting maintenance to a more proactive integrated diagnostic system. This has become so, because detecting and fixing fault(s) on one gas turbine sub-system can trigger false fault(s) indication, on other component(s) of the gas turbine system, due to interrelationships between data obtained to monitor not only the GT single component, but also the integrated components and sensors. Hence, there is need for integration of gas turbine system diagnostics. The purpose of this paper is to present artificial neural network diagnostic system (ANNDS) as an integrated gas turbine system diagnostic tool capable of quantifying gas turbine component and sensor fault. A model based approach which consists of an engine model, and an associated parameter estimation algorithm that predicts the difference between the real engine data and the estimated output data is described in this paper. The ANNDS system was trained to detect, isolate and assess component(s) and sensor fault(s) of a single spool industrial gas turbine GT-PG9171ER. The ANN model was construed with multi-layer feed-forward back propagation network for component fault(s) and auto associative network for sensor fault(s). The diagnostic methodology adopted was a nested network structure, trained to handle specific objective function of detecting, isolating or quantifying faults. The data used for training, and testing purposes were obtained from a non-linear aero-thermodynamic model using PYTHIA; a Cranfield University in-house software. The data set analyzed in this paper represent samples of clean and faulty gas turbine components caused by fouling (0.5% - 6% degradation) and sensor fault(s) due to bias ($\pm1\%$ - $\pm7\%$). The results show the capability of ANN to detect, isolate (classification) and quantify multiple faults if properly trained.

Keywords: Artificial Neural Network; Single Component Fault; Sensor Diagnostics

NOMENCLATURE

ANNDS	Artificial Neural Network Diagnostic System
CF	Component Faults
DCF	Dual Component Fault
NF	No Fault
SF	Sensor Fault
SCF	Single Component Fault
PCA	Pattern Classified Accurately
TET	Turbine Entry Temperature

Symbols

$\mathbf{\Delta}z$ Difference

1.0   INTRODUCTION

To date, gas turbines (GT) have been used to produce large amount of useful work for airborne or surface-borne (land and sea) applications [1]. It has evolved to become the most desirable unit application for power generation at base load, and as an industrial prime mover for the oil and gas sector. However, the overall performance of the GT power plant depends on the availability and performance of its components. Fault(s) on any of the gas turbine subsystem can result into performance or mechanical failure [2,3] of the subsystem(s) which can lead to unexpected outages, low availability and reducing the life cycle cost of the power plant.

The increasing need for gas turbine (GT) engine performance, availability and reliability, has led to several researches on engine health monitoring systems (for example [4]), which can cater for fault detection, isolation and quantification in gas turbine subsystems. To mitigate any negative effect on the GT during operation, fault diagnostic system(s) and health monitoring have been widely used; which is a synchronised concept of data gathering, analysing and development of an action pattern expected to accurately monitor, detect, isolate and quantify the magnitude of fault(s) via its output results. They provide an insight into gas turbine components conditions, revealing possible faults or malfunctions of measurement and control systems such as fouling, erosion, foreign object damage and sensor bias or uncertainty.

However, over the years, the role of diagnostic systems in gas turbine operations has changed from supporting troubleshooting maintenance to a more proactive performance-based [5] integrated diagnostic system [6] . This has become so, because detecting and fixing fault(s) on one gas turbine subsystem could trigger false fault(s) indication on other component(s) of the gas turbine system, due to interrelationships between data obtained to monitor not only the GT single component, but also the integrated components and sensors [7]. Hence, developing a model which integrates the different gas turbine subsystem as described in reference [8] provides an incorporated information about the severity of the GT components fault(s) or instrumentation malfunctions from the knowledge of measured parameters taken along the engine's gas path.

To this end, various engine health monitoring technique such as linear gas path analysis (GPA) [5], have been explored in the past [5]. Rule based expert system(s) have also been investigated for the task mentioned but limitations on handling extensive database of rules and the accuracy of these rules has made its application susceptible. However, several artificial intelligent (AI) based tools have been proposed as alternatives [9,10].

Artificial Neural Network (ANN) is one of such artificial intelligence based tool considered suitable for health condition monitoring of gas turbine (GT) power plants subsystems [6,11]. Artificial Neural Network (ANN) can learn patterns via proper adaptive training [4]. Due to this feature, it is well suitable for modelling non-linear and complex processes of gas turbine engine condition monitoring. Its approach circumvents most of the fundamental difficulties mentioned in preceding paragraph and emerges as a potential tool to carry out modular fault isolation, regression and general estimation problems [12].

In this paper, a diagnostic system using the Artificial Neural Network is presented and has been applied to a single spool industrial gas turbine; a variant of GT-PG9171E for an integrated component(s) and sensor fault(s) diagnosis. The diagnostic system is trained with data set obtained from a non-linear aero-thermodynamic model using PYTHIA; a Cranfield University in-house software. The data set represented samples of clean and faulty gas turbine components caused by fouling and sensor fault(s) due to measurement uncertainty. Changes in the measured parameters reflected changes in the component characteristics; hence, using ANN model to represent

the non-linear interrelationship between them, the different faults under consideration were diagnosed. The results produced from the nested structured ANN diagnostic model are provided and analyzed for discussion.

1.1   Theoretical Basics of Artificial Neural Network (ANN)

A brief description of ANN approach [8,13] is provided as follow;

ANN model employs similar concept of the human neuron to reproduce a relationship between inputs and outputs of linear or non-linear systems [9,14]. It is a set of mathematical model in form of multi-dimensional polynomials that mimics the neural structure of the human brain. It consists of several numbers of interconnected artificial neurons with linear or non-linear transfer functions and is well capable of predicting non-linear behaviour of a system. It learns this relationship through several adaptive iteration processes (training). Hence, they can be harnessed to predict both component and sensor faults when properly trained. The training process of a network involves a continual readjustment of the inter neuron weightings until the error function is minimised; that is to say, training of network is stopped when either the objective function that defines the error has been reduced to the desired level [15–17].

The ANN model for a GT diagnostic system is construed as series of weighted inputs to a processing unit which sums the inputs and decides whether the sum is greater than its threshold level as shown in figure 1
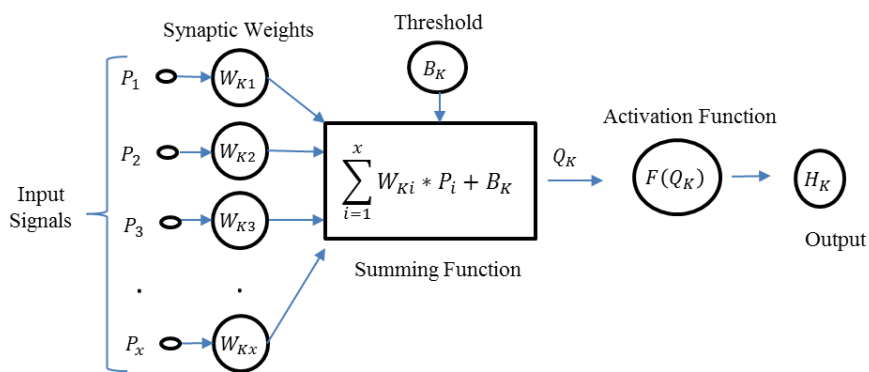

Figure 1 Artificial Neural Network Diagnostic Model

$$Q_K = \sum_{i=1}^{X} W_{Ki} P_i \ + \ B_K \qquad\qquad \dots (\quad 1 \quad)$$

$$H_K = \mathfrak{f}(Q_K) \qquad\qquad \dots (\quad 2 \quad)$$

The scalar input data obtained from the engine model represented as P_i is transmitted via synapses that multiply its strength by scalar weight W_{Ki} to yield the scalar product$(W_{Ki} \ P_i)$. When the bias B_K is added to the system, the argument produces a scalar summation function (Q_K). This summation function becomes the argument of the activation function f also known as the transfer function determining the characteristics of the ANN.

ANN is trained with data captured during the clean baseline and faulty engine operation of the GT. Any reasonable observed difference between the predictions by this trained and the actual measured values of parameters in the plant are indications of a fault or degradation of the component or instrumentation.

The number of neurons and layers in an ANN model depends on the degree of complexity of the system dynamics. The performance of the network is improved by making aware of its specified output(s) through a feedback loop which consist of a transfer function. The performance feedback loop is used to adjust the network parameters in order to improve the system output prediction with respect to the desired goal [18]

The training process in ANN networks can be supervised or unsupervised, depending on whether the targeted output is specified or not during the learning period. In the supervised case, the input and output is usually mapped, while in unsupervised learning, the network clusters similar input data sets.

2.0   FORMULATION OF THE DIAGNOSTIC PROBLEM

The problem is to set up an ANN model which provides diagnostics to both components and sensor faults of a single-shaft gas turbine. Fault(s) is any unexpected changes in the functionality of a system which may be traced to a failure in a physiccal component. In this paper, we considered faults that affect the compressor and turbine as well as six sensor probes. In the present analysis, the goal of the diagnostics is to explore the capability of ANN to detect, isolate and quantify the presence and nature of changes in the condition of the components of a referenced single-shaft gas turbine, caused by deterioration and sensor measurement malfunction. The diagnostic method (ANN) seeks the changes in the engine components by exploiting the way its outputs differ from their values in a clean or healthy state. The expectation is that the diagnostic method should be capable of detecting, isolating, and quantifying integrated faults (component and sensor fault doused with noise) in a gas turbine.

2.1   GT Component Faults

The reference engine is single-shaft gas turbines that consist of a compressor, combustor and turbine. When gas turbines deteriorate as a result of fouling or erosion, the effect is manifested in the performance of the gas turbine component efficiency and mass flow capacity reduction [2,3]. In the absence of real faulty data, the compressor and turbine component faults was simulated by implanting fault onto the adaptive model of the reference plant. The relationship between the physical deterioration and the simulated is realised by setting certain ratios of the component efficiency and mass flow capacity which are a representative effect of compressor fouling and turbine erosion. The combustor is excluded in this analysis because its efficiency is relatively stable with time. Degradation does not reflect adequately on the measurement parameter.

The level of fault implanted for the compressor and turbine is shown in Table 1. This is implemented in simulation tool by reducing the component efficiency and flow capacity as specified with 0.5% stepwise. For the turbine, the flow capacity was implemented with fault by increasing it to represent turbine erosion.

Table 1 Compressor and Turbine Faults

	Fault Level Implanted (%)
Compressor Flow Capacity Γ_C	$0.5\ to(-6)$
Compressor Isentropic Efficiency (η_C)	$0.5\ to(-6)$
Turbine Flow Capacity Γ_t	$0.5\ to(+6)$
Turbine Isentropic Efficiency (η_t)	$0.5\ to(-6)$
Combined	0.5 to (±4)

2.2   GT Sensor Faults

Modern power plants depend on accurate and reliable sensor readings for the purposes of engine control and monitoring [19]. When sensors fail due to instrument degradation, measurement errors become unavoidable during gas turbine operation, and it can force the power plant or component into non-optimal performance and unavailability. Hence, the optimal prompt detection of sensor fault(s) is important to the functionality and availability of the plant unit. In this work, sensor faults were implanted onto the adaptive engine model with the aim of applying ANNDS to detect, classify and quantify the faults implanted. Six measurement set selected were doused with noise using equation 3

$$FS = Sb + \Delta Sb \qquad \qquad …(\quad 3\quad)$$

Where FS , is the measurement fault, Sb, is the measurement baseline without noise and ΔSb, is the level of noise or bias implanted.

The level of fault simulated for this study and the non-repeatability range of the sensors for which they can be considered as producing faulty readings is shown in Table 2

Table 2 Sensor Fault Characteristics

	Descriptions	Non-Repeatability Range	Fault Level Implanted (%)
P3	Compressor Discharge pressure	±0.5	$\pm(1\ to\ 7)$
T3	Compressor Exit Temperature	±1	$\pm(1.2\ to\ 7)$
FF	Fuel Flow	±0.5	$\pm(1\ to\ 5)$
P7	Turbine Discharge pressure	±0.5	$\pm(1\ to\ 7)$
T7	Turbine exit Temperature	±1	$\pm(1.2\ to\ 7)$
PCN	Shaft Rotational Speed	±0.1	$\pm(0.2\ to\ 3)$

2.3   Brief Description of Referenced Gas Turbine

The modelled engine used for this study is a single-shaft gas turbine with output power of 126.1MW. The engine was designed for 50Hz, 3000rpm nominal speed coupled directly to a 2-pole synchronous generator. It has the design features and solutions of the GE-MS9001E family introduced in the 1970s. The compressor is an axial flow type which has 17 stages with an overall pressure ratio of 12.6:1. Air is extracted from the 5th, 11th and 17th stage of the compressor unit for cooling and sealing rotor bearings, for start-up and shutdown pulsation control, and for turbine blade cooling. The combustion unit utilizes a reverse flow type and a 14 can-annular combustion chamber arranged around the periphery of compressor discharge casing, and incorporated with DLN. The turbine has 3 stages with internal cooling. The schematic and operating parameters of the model engine is shown in figure 2

	Specifications	Predicted	Variation
Output Power (MW)	126.1	126.1	0
Thermal Efficiency (%)	33.8	34.1	-0.3
Pressure ratio	12.6	12.6	0
EGT (°K)	816	816.22	-0.22
Heat Rate (KJ/KWh)	10640	10645.28	-5.28
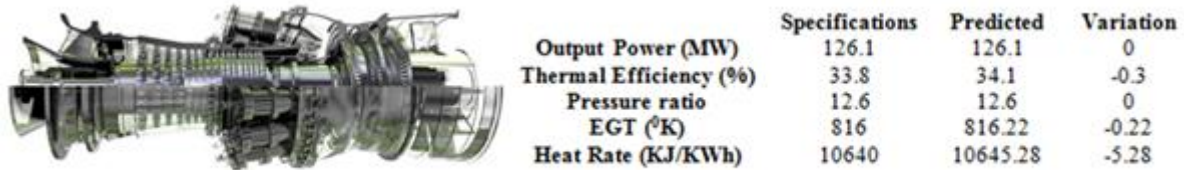
Figure 2 Overview of Reference Gas Turbine (similar to GE PG9171E) [20]

3.0   METHOD OF ANALYSIS

In order to assess the health of the modelled GT engine shown in figure 2 and ultimately provide a diagnosis concerning any detected fault(s), it becomes important to have data that relate the engine gas path measurements with the independent performance parameters under a healthy (baseline) and number of faulty conditions that covers all case of interest. Hence, in the absence of real time engine data, it became necessary to use a gas turbine performance model to generate the required data for application onto an artificial neural network diagnostics system (ANNDS). For this purpose, a simulation program called PYTHIA [21], developed at Cranfield University was used to formulate an adaptive performance model and to estimate the health indices of the reference engine at clean or healthy (baseline) and for the effects of the engine component deterioration, as well as sensor faults.

To this end, the following steps were taken to achieve the set goal of integrated diagnostic using ANNDS

1. Adaptive thermodynamic modelling of reference gas turbine engine.
2. Optimum measurement set selection in order to determine the optimum combinations that would be effective to diagnose the desired faults.
3. Faults implantation in the engine model and generating data to cover all possible fault matrixes in the compressor, turbine and sensor malfunction.
4. Development of ANN diagnostic structure of data flow
5. Training, testing and analysing the performance

In this study, all networks were trained using supervised learning. Training of the ANN was done in MATLAB neural network toolbox.

3.1   Data Set Acquisition

The purpose of data acquisition is to obtain performance parameters that represent all classes of faults under analysis, through the sensor probes around the engine gas path and to translate the acquired data into formats that would be useful for the diagnostic system. The proper selection of the sets of input parameters for accurate prediction of the sets of output parameters is vital for any ANN diagnostic system. Hence, an approach to obtaining the right sets measurement-set was achieved by observing the sensitivity of measurement parameters to changes in the component health indicators (Flow capacity and efficiency). Measurement parameters with high sensitivity are desirable because they are easy indicators of deterioration and are not easily susceptible to noise or uncertainty [7,22]. Figure 4 shows the location of the sensor probes selected for acquisition of both clean and faulty data to be used for GT-PG9171ER diagnostics. Faulty data generated covered all classes as discussed in section 2.1 and 2.2. The faulty data were generated at 90% shaft power since the engine is not expected to perform at full power in operation. Other baseline conditions considered during this process was

ISO SLS condition and TET was used as engine handle. All data generated were normalised under the same manageable range for easy assessment using equation 4.

$$\Delta Z = \frac{\{Z_p - Z_b\}}{Z_b} \times 100 \qquad\qquad \dots (\quad 4\quad)$$

Where, Z_b, is the value at established baseline condition, and, Z_p, is the measured or calculated value

In order to carry out the diagnostic, 4 set of data are required

- Training data
- Target output data
- Validation and Test data

In total 25008 sample points generated, 65% was used for training purposes, while 35% was used for validating and testing purposes. Data were processed for use according to the objective function of each network in the ANNDS. Table 3 shows a breakdown of data acquired for clean and faulty conditions.

Table 3 Breakdown of Data Processed

	Number of Sample Patterns
Clean	1000
Compressor	4320
Turbine	4320
Compressor &Turbine	8192
Sensors	7176
Total	25008

3.2   ANN Fault Diagnostic System Description

The concept of ANNDS is to recognise a fault signature if one exists within the engine measurable parameters. If a fault signature is recognised, it must then be able to determine which component or sensor the fault signature relates to. Once the component or sensor is identified, the diagnostic system must quantify by providing prediction on the level of fault.
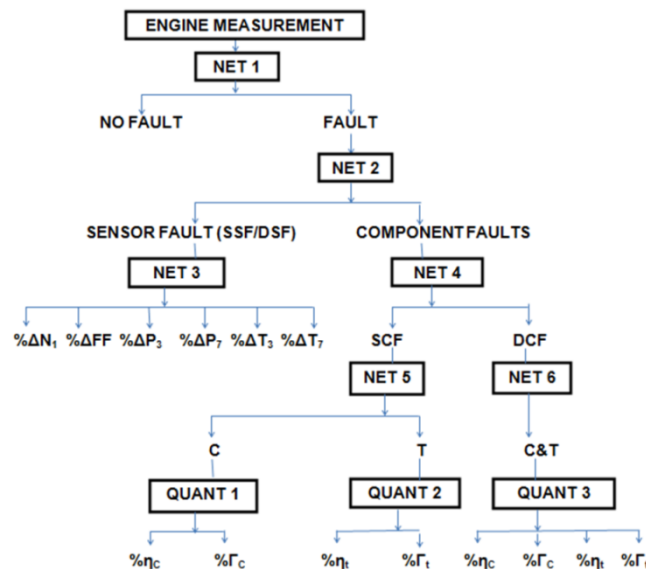
Figure 3 Nested Structure of ANNDS for GT-PG9171ER

The ANN diagnostic structure used for this study is shown in figure 3. Using a single network structure will be unrealistic because of the number of objective and the size of the data library required for this analysis. Thus, a nested structure was used [15], so that each network is assigned an objective function; thereby making the diagnostic tool very efficient. In the first network denoted as NET1, all the normalised data generated for both the components and sensors are fed into it, where they are classified as 'faulty or no fault' data. All patterns detected as faulty are fed onto the NET2, while the 'no fault' data require no further diagnostic action. This implies that the input met the required output threshold of clean data. At the NET2, input data detected are

classified as sensor or component faults. If sensor faults, the data is fed onto NET3 for quantification. A deviation of the quantified data from the clean data provides an indication on the amount of bias or noise present in each sensor. On the other hand, data classified as component faults in NET2 are fed onto NET4. At NET4, the data patterns consisted of single and dual component faults. The objective function of NET4 is to classify the faults and pass it onto NET5 or NET6. Single component fault are detected by NET5, where the patterns are isolated as either compressor or turbine fault. Successfully isolated component faults are passed onto the QUANT1 and QUANT2 for quantification of deviation from baseline by determining changes in component efficiency and flow capacity degradation. Similarly, NET 6 passes the dual component fault onto QUANT3 for further quantification of deviation.

The basic requirement for each of the network defined is to have adequate representation capacity of faults which are proportional to the number of parameters selected, and availability of sufficient training data that will cover all the expected operatinfg ranges of the network
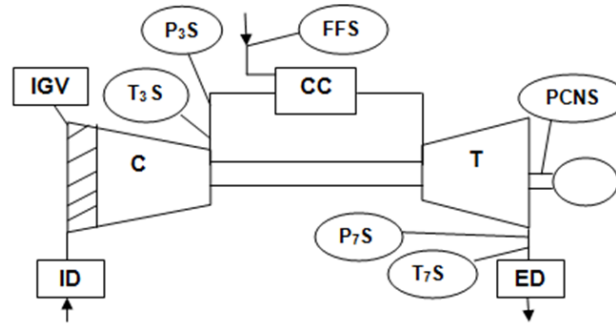
Figure 4 Sensor probe location

3.3   Network Architecture, Training and Algorithm
The network architecture defines the pattern in which the neurons of the network are organised. This sudy utilised the multilayered feed-forward back propagation (MLFFBP) architeture for component fault and the auto associative feed-forward neural network (AAFFNN) architecture for sesnor fault diagnostic. During the MLFFBP training process, inputs data are transmitted through the network, layer by layer, and a set of output is calculated by the activation function. The calculated output is compared with the target output values. Error from this comparison of predicted (calculated output) and target output is feedback into the network which prompt a dynamic adjustment of the weight and bias in order to reduce the level of error. This iterative process continues until a mininum acceptable level of error is achieve, which mean that the output response is closer to the target set. Each iteration of the whole set of data is called Epoch. The dynamic adjustment of the synaptic weight is corrected using equation 5. The number of layer and output node used in this work is set based on the task to be performed by each NET in the ANNDS structure.

$$\Delta W_{ij}(n)^{(m)} = \eta \times d_j(n) \times y_i(n) + \propto \Delta W_{ij}(n)^{(m-1)} \qquad \dots (\quad 5\quad)$$

Where $\Delta W_{ij}(n)$ is termed the weight correction, η is the learning rate parameter, $y_j(n)$ is the input signal of the j node. $\delta_j(n),$ is the local gradient, α is the momentum coefficient and m is the number of iterations

The major distinctive feature of the AAFFNN is that it contains a bottleneck layer which has a non-linear transfer function and both the input and output values are the same. All the noise filtering is achieved at the mapping part (between the input and the bottleneck layer). After the intrinsic states are determined from the mapping process, a demapping part is followed by decoding the nodes of the bottlenec to the output layers.

The non-linear sigmoid transfer function and binary threshold function was used for the layers depending on the network objective.The sigmoid transfer function takes the input values between plus or minus affinity and squashes its output into a range between 0 and 1 described by equation 6, while the binary threshold limits the output to either 0 or 1 represented with equation 7

$$H_K = f(Q_K) = \frac{1}{(1 + exp(-P_i Q_K))} \qquad \dots (\quad 6\quad)$$

$$H_K = f(Q_K) = \begin{cases} 0, & if \ Q_K < 0 \\ 1, & if \ Q_K \geq 0 \end{cases} \qquad \dots (\quad 7 \quad)$$

In the learning process, in order to increase the learning speed and maintain stability, the Lavenberg-Marquardt learning rule and scaled conjugate gradient learning rule was used [13]

3.4   Network Performance

The performance of the network is assessed based on the generalisation ability to validation and test data, and the performance index. Some of the performance index used is defined as follow:

- **Mean Square Error (MSE)**
  This error is calculated as average difference between the target output and the network output (predicted).

$$MSE = \frac{1}{T} \sum_{K=1}^{T} E_{rr}(K)^2 = \frac{1}{T} \sum_{K=1}^{T} (Y(K) - H(K))^2 \qquad \dots (\quad 8 \quad)$$

  Where($Y(K)$, is the network output,$H(K)$, is the target output and T is the number of output layer neurons.

- **Root Mean Square Error (RMSE)**
  This is gives a general purpose error metric for numerical prediction. It is given by the square root of the MSE

$$RMSE = \sqrt{\frac{1}{T} \sum_{K=1}^{T} E_{rr}(K)^2 = \frac{1}{T} \sum_{K=1}^{T} (Y(K) - H(K))^2} \qquad \dots (\quad 9 \quad)$$

- **Confusion Matrix (CM)**
  This shows the number of patterns classified accurately (PCA) and the number of patterns classified inaccurately (PCI). It is represented in percentage.

- **Regression**
  This shows how closely fitted the network output data is to the target output. A regression value close to 1 justifies the network trained.

- **Standard Deviation (σ)**
  This is used to assess the distribution of prediction errors in the quantification networks; that is difference between the target values and predicted values.

4.0   RESULTS AND DISCUSSION

This section presents a brief description on how each network is trained to satisfy the performance of the ANNDS, where NET1, NET2, NET4, NET5, NET6 are for classification, while NET 3, QUANT1, QUANT2, QUANT3 are for quantification of the faults.

4.1   NET1

The objective of this network was to accurately classify all the engine measurement data patterns into faulty or a 'no fault'. This network was trained with 25008 data from 6 measurement sets, consisting both faulty and clean data as shown in Table 3. The target output for this network was set as a binary (0, 1). When there is 'no fault' the target output becomes '0' and when there is fault, the output is set as '1'. After 220 iterations (Epoch) of training, validation and test using different architectures (for example 6-15-1), the best classification performance converged with the least MSE of 0.0075, generalisation classification ability of 99% (pattern classified accurately) and 1% misclassified. From the 99% classified accurately, NET1 detected 95.7% (23923) patterns as faulty and 3.3% (837) as clean ('no fault') based on Table 3. The result from testing the network is shown in figure 5 to figure 7, which demonstrated its capability to handle large data in the presence of noise or bias, and still able to satisfy the task objective.

4.2   NET2

The established faulty pattern from NET1is passed onto this network where isolation of the fault pattern is classified as either sensor or component fault. A total of 24008 samples were used for training, validation and testing of this network. The target output was set at (1 0) for faulty components and (0 1) for faulty sensor. Similar to the NET1, scaled conjugate gradient learning rule was used to map the input to the target output. The result of the network testing after 221 training iteration is shown in figure 8 to 11. 97.5% were classified accurately which consisted 29.9% (7168) as sensor faults, 67.7% (16232) as component faults and 2.5% (608) was not recognised (misclassified) in any fault class.
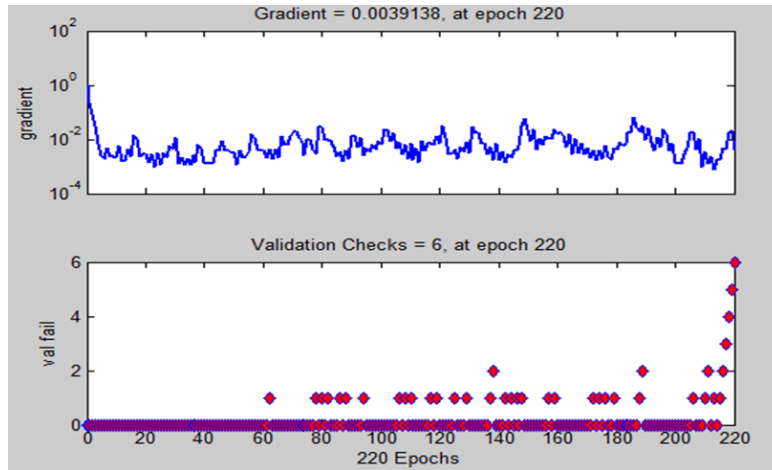
Figure 5 Training State of NET1
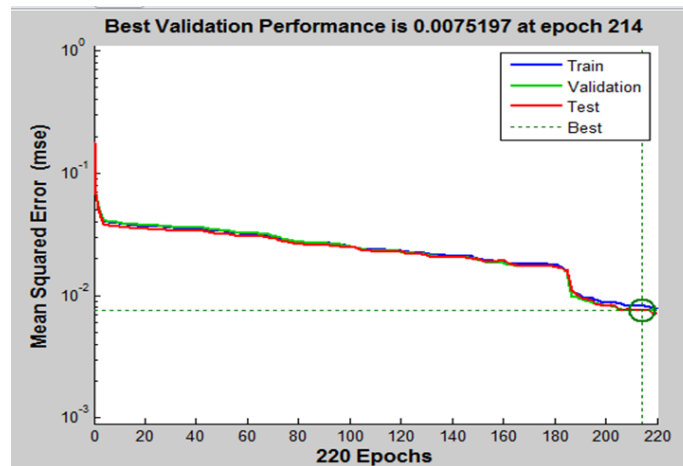
Figure 6 Validation of NET1
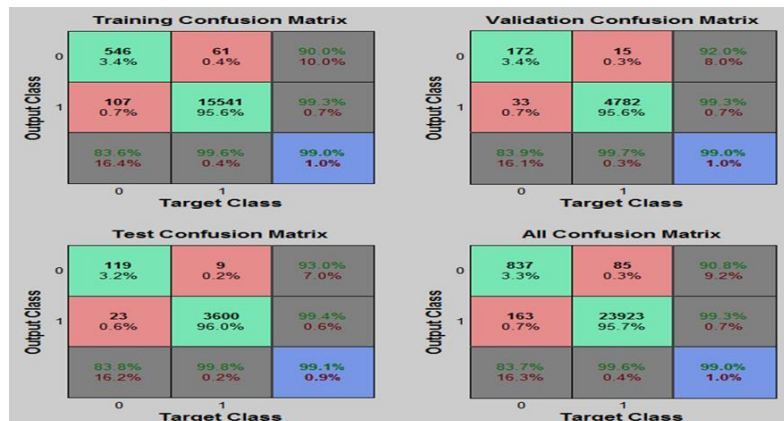
Figure 7 PCA of NET 1
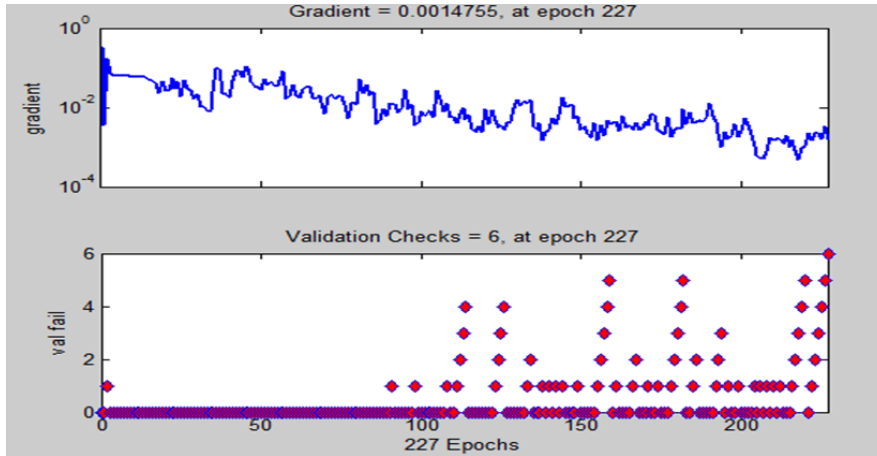
Figure 8 Training State of NET2
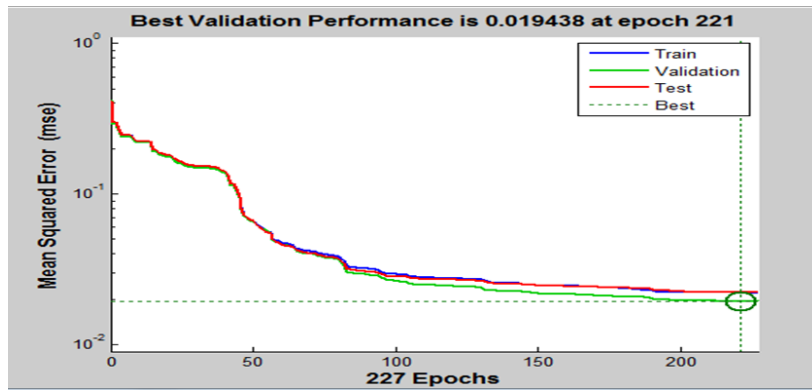
Figure 9 Validation of NET2
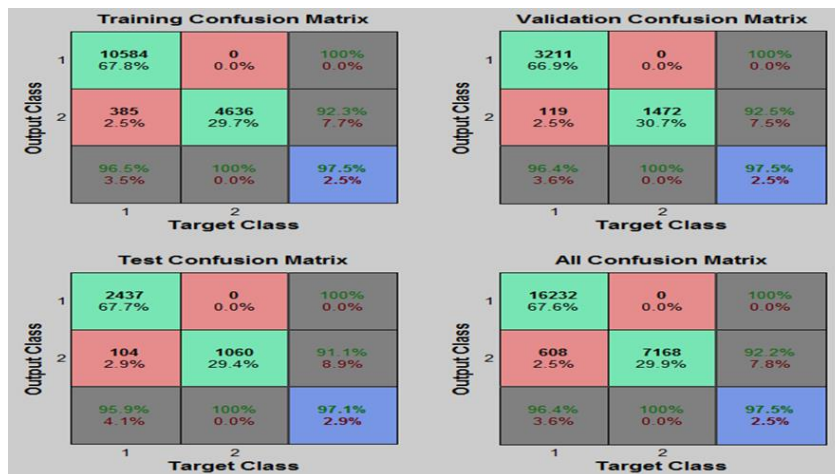
Figure 10 PCA of NET2

4.3   NET3

As previously described, this network isolates the sensor faults and quantifies the amount of data from each sensor declared faulty that lies within its threshold. AANN with Lavenberg-Marquardt learning rule was used to train this network. The number of nodes for the input and output layers were determined by the size of the input vector. Hence, 6 nodes (neurons) representing the selected measurement sets was used as the input and target parameters. Determining the appropriate number of nodes for the hidden layer was not straight forward, because few nodes implies that the network cannot properly identify the non-linear correlations between the input

values, hidden nodes and output. Too many nodes can also lead to 'overfitting' the network. However, with good engineering judgement and after several trials, a 6-15-3-15-6 architecture was chosen to give the best isolation performance and minimum error. A total of 7176 faulty sensors measurement was used to training and test purposes. The first step was to isolate each individual sensors faults (P3, T3, FF, P7,T7, PCN) from the set. This required NET3 to perform classification task. The results showed 83% were accurately classified and 17% misclassified with an MSE of $3.2 * 10^{-8}$.

The next step is to quantify the faulty sensor data. To achieve this, two thresholds were fixed on the difference between the input and the output vector. When the MSE is between the first and the second threshold, then, the sum of the erros are weighted by the measurement non-repeatability, and compared. If error is larger than the threshold., then the larger error to non-repeatability ratio isolates the sensor error. The target output was set at values obtained when engine was not with noise or bias. Hence, the performance is judged based on the percentage of outputs that were established within the noise level.

This process was repeated for all the sensors. To avoid repetition, only result of T7 sensor is presented in Table 5. Samples implanted with fault should fall outside its error threshold of $\pm1.0\%$, but within the fault level implanted shown in Table 2. The results shows that average of 93.6% of data fell outside the error threshold which are indications of faulty sensor of data. correctly detected but are meant to fall within the fault level were misquantified.
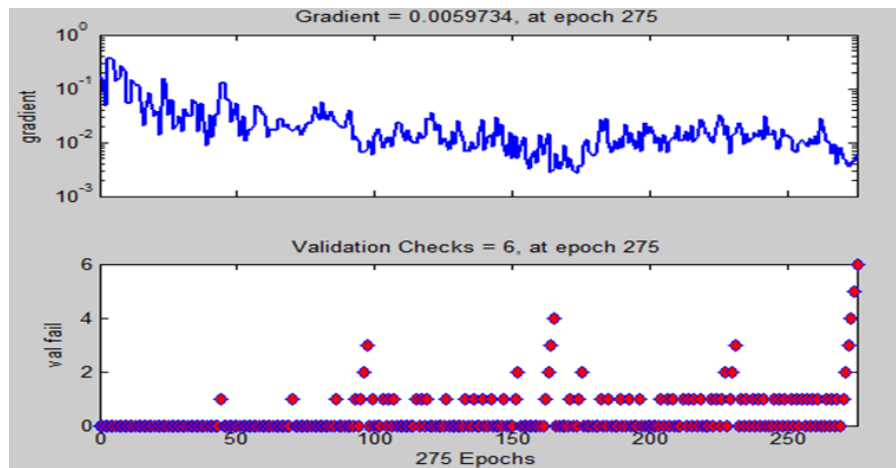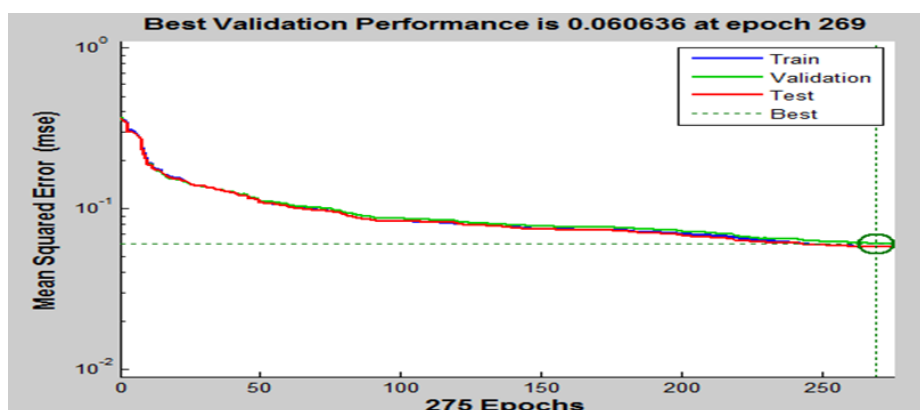

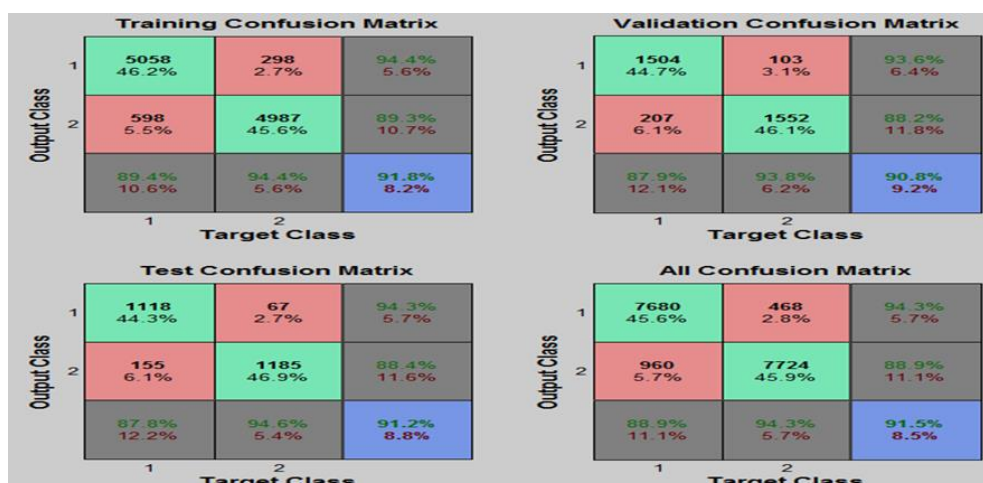Figure 11 Training State of NET4

Figure 12 Validation of NET4

Figure 13 PCA of NET4

4.4   NET4

This network was trained to isolate the type of component faults as discussed in section 3.2. A total of 16832 samples were used to training, validation and testing. Two output node was set as target output, represented as (1 0) for single component fault (SCF) and (0 1) for dual component faults (DCF). Similar to previous discussion, architecture 6-18-2 exhibited the best trained performance with 45.6% of input classified accurately as SCF, 45.9% as DCF and 8.5% misclassified with an MSE of 0.0606. The results of its generalisation justify the network ability to isolate component faults as shown in figure 11 to figure 13.

4.5   NET5 & NET6

Both networks were trained with scale conjugate gradient learning rule. For NET5, the target output was set similar to NET4, but in this case (1 0) for compressor fault and (0 1) for turbine fault. The performance of NET5 showed 37.6% PCA for compressor, 41.7% turbine faults and 20.7% misclassified with an MSE of 0.1251. NET6 was designed for pattern recognition of DCF with a target output set at (1 0) where 1 for faulty DCF and 0 for 'not a DCF fault'. Data from both networks are further fed onto the QUANT network for quantification of faults. NET5 and NET6 results are shown in Table 4

4.6   QUANT1, QUANT2 & QUANT3

The goal of these fault quantification networks is to be able to approximate an output based on a set of received data. The networks were trained to detect and estimate the magnitude of deterioration in the faulty component(s) in terms of isentropic efficiency and flow capacity degradation. QUANT1 network is to quantify compressor faults, QUANT2 for turbine faults and QUANT3 for dual component faults. The processes of these networks are similar, hence to avoid repetitions; QUANT 1 is described alongside with other QUANT network and results presented according to the objective function of each networks. The MATLAB "*nftool*" with FFBP and Levenberg-Marquardt algorithm was used to train each network. Similar to previous discussions, different architectures were tried for each QUANT network to obtain the best network performance. Each QUANT target output also corresponds to the level of deterioration of the component(s) in terms of changes in isentropic efficiency and flow capacity, which covers the whole range of implanted deterioration as described in Table 1.

The assessment of each QUANT network was achieved using statistical correlations between the network output obtained and the target output. Relative Error which gives the normalized difference between both outputs mentioned was calculated for isentropic efficiency and flow capacity respectively. The mean and standard deviation of the relative errors for each performance deterioration (η and Γ), was also calculated and direct comparison between the isentropic efficiency and flow capacity was established by obtaining the percentage relative error as shown in figure 14 and 15.

The value of the standard deviation obtained, was used to determine the amount of data that lies within the 1σ, 2σ and 3σ of the mean error. Estimations with the lowest standard deviations are considered favorable to predict the magnitude of component deterioration.

The results of QUANT1 presented in Table 5 after different architectures were tested showing that architecture 6-18-2 had the least standard deviation and predicted about 95% of the data within the 2σ for both efficiency and flow capacity. Plotting the Histogram of the percentage relative error for both efficiency and flow capacity

of the network as presented in Figure 14 and 15, showing how much data lie close to the average error. This is represented by values close to the zero percent mark in the histogram.
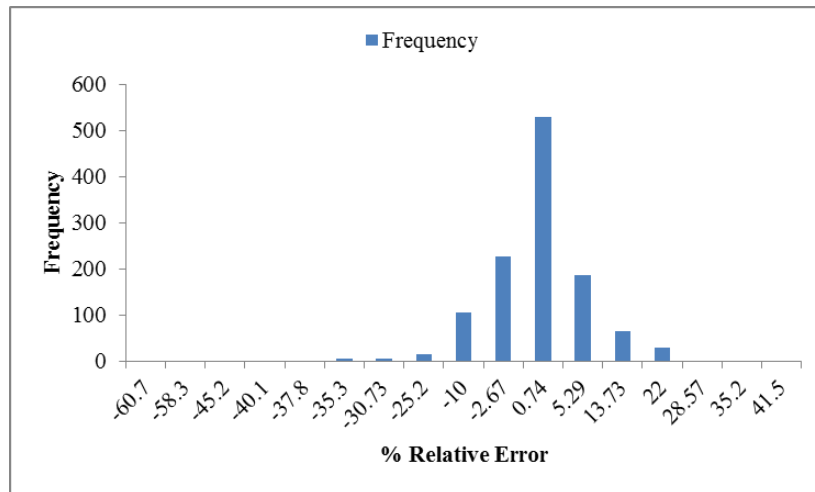

Figure 14 Histogram of Relative Error for QUANT 1 Network (6-18-2) Predicting Flow Capacity
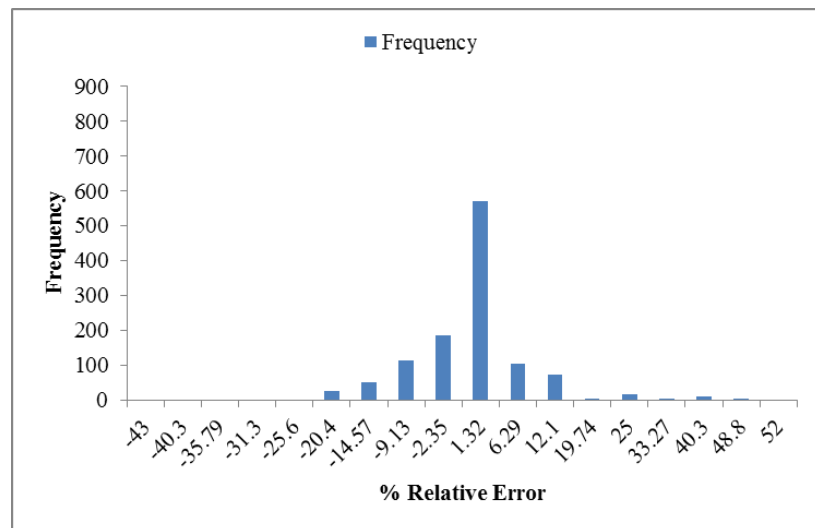

Figure 15 : Histogram of Relative Error for QUANT1 Network (6-18-2) Predicting Isentropic Efficiency

It can be seen that the QUANT1 network shows better prediction of flow capacity than the isentropic efficiency, because of cases with large relative error of approximation for isentropic efficiency.

A summary of the ANNDS results are presented in Table 4 and Table 5 which shows the performance of the classification networks and the quantification networks. NET 1, NET 2, NET 4, NET5 and NET 6 are classification networks while QUANT1, 2, 3 and NET 3 are quantification networks. The classification networks play important roles in the nested ANNDS, if the classification doesn't give satisfactory result; it becomes difficult to obtain a meaningful quantification of fault level. The classification networks were assessed by success rate of recognition and isolation of sample patterns. Figure 16 showed that the classification network achieved over 75% accuracy. NET 5 performed the least, because of the difficulty assessing fault severity when more than one component degrades in similar magnitude of fault signature. The quantification networks were not assessed based on PCA but on standard errors and a comparison of their performance is shown in Figure 17. The prediction of diagnosis is represented with a 2σ confident interval, which was computed from large amount of validation samples in the training period. A lower 2σ of error means that the network can predict more accurately, while a large 2σ of error means that the confidence interval of this prediction would be spread, hence a poor network estimate. The result shows that the flow capacity had better predictions with minimum standard deviations from the mean error than the isentropic efficiency most of quantification networks. This was assessed using 2 standard deviations (2σ) of the relative error between the network output and the target output as

presented in Figure 17. The results also shows that the quantification of single component faults where more accurate than dual component faults. This is because the performance of ANN depends on the complexity of the problem. QUANT2 exhibited the best performance with the least standard error.

The results from NET3 for the sensor fault isolation and estimation that lie between the noise level threshold of $\pm 1.0\%$ and fault level implanted for T_7 was also very satisfactory. The NET 3 performed two objectives: it was trained to isolate single sensor faults from dual sensor faults and was later trained to estimate single sensor fault using T_7 as case study. Two standard deviations (2σ) were also used during analysis of the estimation results. Measurements that fell outside the threshold were those implanted with bias which is an indication of a faulty sensor.

Table 4 Performance of Classification Network

	Network	Selected Architecture	Performance		$\overline{MSE}$	RMSE
			$\overline{PCA}$ (%)			
			NF	**F**		
1	NET 1	6-15-1	3.3	95.7	0.0075	0.0885
			SF	**CF**		
2	NET 2	6-15-2	29.9	67.8	0.0194	0.1465
			SCF	**DCF**		
3	NET4	6-18-2	45.6	45.9	0.0587	0.2422
			C	**T**		
4	NET 5	6-10-2	37.6	41.7	0.1252	0.3537
5	NET 6	6-10-2	100	-	0	0

Table 5 Performance of Quantification Network

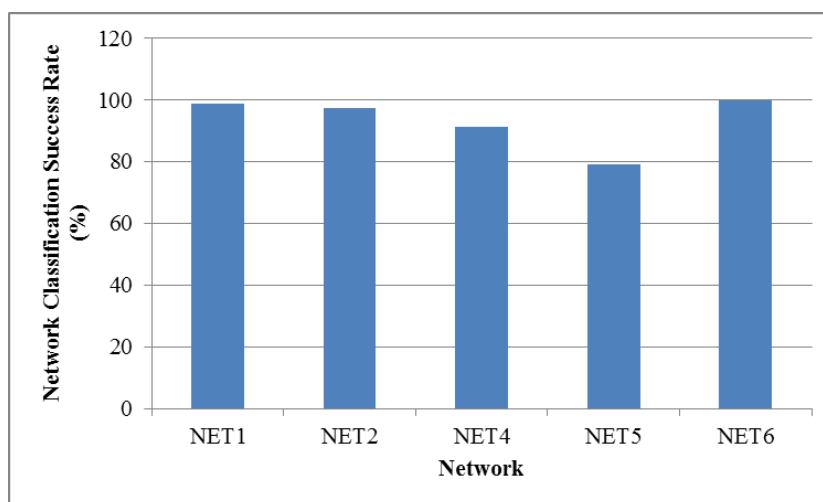|	Network	Selected Architecture	Performance	
			$\overline{MSE}$	RMSE
1	NET 3 Isolate	6-15-3-15-6	4×10^{-8}	0.0002
2	NET3 T_7	6-15-3-15-6	0.0475	0.2141
3	QUANT1	6-18-2	0.0145	0.1207
4	QUANT2	6-15-2	0.0082	0.0906
5	QUANT3	6-15-4	0.0368	0.1919

Figure 16 Generalisation Ability of Classification Network
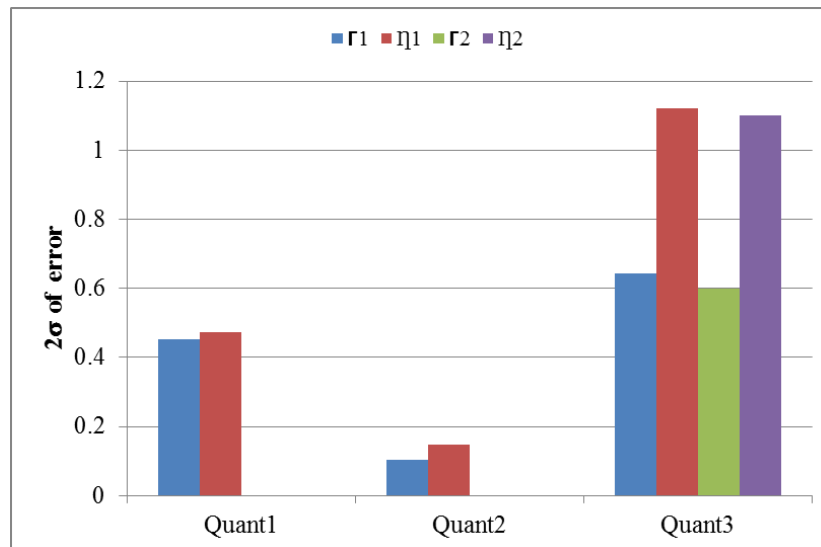
Figure 17 Generalisation Ability of Quantification Network using 2σ of prediction error

5.0   CONCLUSION

An ANNDS nested diagnostic system has been presented in this paper as a tool for EHM of an industrial gas turbine PG9171ER. The level of accuracy obtained through the application of the nested ANN provided much benefit to its performance when compared with just a single network performing several fault isolation or detection functions. The overall performance of the nested structure depended on the combinative capability of each individual NET. The quality of the diagnostics results is influenced by the quality of the data obtained from the engine model. To this end, using PYTHIA was a useful tool for simulation of fault(s), automatic interaction with component data and the variations of faulty samples needed for the engine model diagnostic purposes. This was achieved by implantation of component(s) and sensor faults representing deterioration in efficiency, flow capacity and instrumentation error. The component faults implanted on the model, ranged from -0.5% to -6.0% for efficiency and 0.5% to 6.0% for flow capacity. Three classes of component fault(s) were simulated and a total of 25008 data were processed for diagnostic purposes of training, validation and testing of network. The results of the generalisation ability of the classification and quantification of the ANNDS showed a high level of success rate (above 80%) for NET1, NET2, NET4, and NET6. Quant1 prediction also demonstrated ability to quantify accurately with data falling within the range (-0.5% – (-6.0%)) implanted fault.

Finally, from the application results for diagnostics of the GT-PG9171ER industrial gas turbine using ANNDS, it is to draw conclusion that the proposed diagnostics system was able to perform diagnostic task of detecting and quantifying faults such as fouling and erosion on the GT components and faulty sensors. However, the limitation of the diagnostic model is the capability of handling complex dual component fault of similar fault signature.

ACKNOWLEDGMENTS

REFERENCES

1.   Giampaolo T. Gas Turbine Handbook Principles and Practice. 3rd edn. New York: Fairmont Press Inc.; 2016.

2.   Diakunchak IS. Performance Deterioration in Industrial Gas Turbines. Journal of Engineering for Gas Turbines and Power. 1992; 114(2): 161. Available at: DOI:10.1115/1.2906565

3.   Meher-homji CB., Chaker M a., Motiwala HM. Gas Turbine Performance Deterioration. 30th

Turbomachinery Symposium, Texas A&M University, Texas. 2001; : 139–176. Available at: http://turbolab.tamu.edu/proc/turboproc/T30/t30pg139.pdf

4.   Kong C., Ki J., Kang M., Kho S. Intelligent Performance Diagnostics of a Gas Turbine Engine. Aircraft Engineering and Aerospace Technology. 2004; 76(4): 391–397.

5.   Li YG. Performance-analysis-based gas turbine diagnostics: a review. Proceedings of the Institution of Mechanical Engineers, Part A: Journal of Power and Energy. 2002; 216(5): 363–377. Available at: DOI:10.1243/095765002320877856

6.   Volponi AJ. Gas Turbine Engine Health Management: Past, Present, and Future Trends. Journal of Engineering for Gas Turbines and Power. 2014; 136(5): 51201. Available at: DOI:10.1115/1.4026126

7.   Stamatis A., Mathioudakis K., Papailiou K. Optimal Measurements and Health Indices Selection for Gas Turbine Performance Status and Fault Diagnosis. ASME Journal of Engineering for Gas Turbines and Power. 1992; 114: 209–216. Available at: DOI:10.1115/91-GT-294

8.   Osigwe EO. Application of Artificial Neural Network Diagnostic System on Gas Turbine Components and Sensor Fault Diagnosis. Cranfield University; 2014.

9.   Sampath S., Gulati A., Singh R. Artificial Intelligence Techniques for Gas Turbine Engine Fault Diagnostics. 38th AIAA/ASME/SAE/ASEE Joint Propulsion Conference and Exhibit. Indianapolis: AIAA; 2002. pp. 1–12. Available at: DOI:10.2514/6.2002-4308

10.   Simon DL., Armstrong JB. An Integrated Approach for Aircraft Engine Performance Estimation and Fault Diagnostics. Cleveland, Ohio; 2012.

11.   Loboda I., Yepifanov S., Feldshteyn Y. An integrated Apporach to Gas Turbine Monitoring and Diagnostics. Proceedings of ASME Turbo Expo 2012: Power for Land , Sea and Air. Berlin: ASME; 2008. pp. 1–9.

12.   Lu PJ., Zhang MC., Hsu TC., Zhang J. An Evaluation of Engine Faults Diagnostics Using Artifical Neural Networks. Transactions of ASME, Journal of Engineering Power. 2001; 123: 340–346. Available at: DOI:10.1115/1.1362667

13.   Hegan MT., Demuth H., Beale M. Neural Network Design. Nevada: PWS Publishing Company; 1996.

14.   Fast M., Assadi M., De S. Development and Multi-Utility of an ANN Model for an Industrial Gas Turbine. Applied Energy. 2009; 86: 9–17.

15.   Ogaji SOT., Singh R. Advance Engine Diagnostics Using Artifical Neural Networks. Applied Soft Computing. 2003; 3: 259–271. Available at: DOI:10.1016/s1568-4946(03)00038-3

16.   Zedda M., Singh R. Gas Turbine Engine and Sensor Fault Diagnosis using Optimisation Technique. 35th AIAAA/ASME?SAE?ASEE Joint Propulsion Conference and Exhibit. Los Angeles: AIAA; 1999. pp. 1–10.

17.   Asgari H., Chen X. Artificial Neural Network – Based System Identification for a Single-Shaft Gas Turbine. 2013; 135(September): 1–7. Available at: DOI:10.1115/1.4024735

18.   Ogaji SOT., Singh R., Probert SD. Multiple-sensor fault-diagnoses for a 2-shaft stationary gas-turbine. Applied Energy. 2002; 71(4): 321–339. Available at: DOI:10.1016/S0306-2619(02)00015-6

19.   Mattern DL., Jaw L c., Guo TH., Graham R., McCoy W. Using Neural Networks for Sensor Validation. 34th AIAA/ASME/SAE/ASEE Joint Propulsion Conference and Exhibit. Cleveland, Ohio: AIAA; 1998.

20.   SCA. SCA Technical Specification on GE 9E Frame. 2013. Available at: http://www.scribd.com/doc/163524237/SCA-Technical-Spec-GE-Frame-9E-s-Rev1

21.   Li Y. PYTHIA User's Guide. Cranfield: Cranfield University; 2015. pp. 1–169.

22.   Jasmani MS., Li Y., Ariffin Z. Measurement Selections for Multi-Component Gas Path Diagnostics Using Analytical Approach and Measurement Subset Concept. Proceedings of ASME Turbo Expo 2010: Power for Land , Sea and Air. ASME; 2010.

2017-09-11

Integrated gas turbine system diagnostics: components and sensor faults quantification using artificial neural networks

Osigwe, Emmanuel O.

International Society for Air Breathing Engines (ISABE)